

In contrast, the product distribution for the photolysis of *o*-ACOB depends on the zeolite substrate (Table I). As shown in Table II, sorption of *o*-xylene from the vapor phase highlights the differences in the zeolites. The sorption rate of *o*-xylene into LZ-105 is so small that it must be concluded that virtually all of the *o*-ACOB for this sample is sorbed on the exterior. This conclusion is consistent with the observation that isooctane extraction is able to completely recover the *o*AoA and *o*AB photolysis products. That the *o*A segment is too large to enter the framework channels is consistent with the *o*-xylene sorption results. The absence of BB product in the isooctane wash indicates that it resides within the zeolite framework. We postulate that the molecule *o*-ACOB may be sorbed on the zeolite surface in two orientations, one where the entire ketone molecule is on the outer surface and another where the smaller segment of the ketone intrudes into the channel opening, whereas the larger segment of the ketone must remain on the outer surface.

From Tables I and II we conclude that no *o*-AB is formed within the zeolite framework for LZ-105. The difference between the observed product distributions and those of a solvent random radical coupling can be attributed to rapid B· radical sieving. The sieved B· radicals are inhibited from coupling with *o*-A· radicals which must remain on the external surface. As a result, *o*-A-*o*-A and BB coupling becomes dominant over *o*-AB coupling.<sup>13</sup>

For ZSM-5, because the product distribution is the same as that for random radical couplings, we propose that BB coupling occurs predominately on the external surface, and that BB molecules are sieved into the internal surface after they are formed. For ZSM-11, although the BB coupling/sorption mechanism seems to be operating, there is an excess of *o*-AB formed, because some *o*-ACOB was absorbed prior to photolysis. From the xylene sorption data, the ratio of surface to framework photolysis is expected to strongly depend on the sorption exposure time (Table II) and temperature. Indeed, longer times and higher temperature favor more *o*-ACOB entering the framework resulting in a greater cage effect and *o*-AB, therefore, becomes the major product.<sup>14</sup>

In summary, the photolyses of *o*-ACOB in the presence of pentasil zeolites follow strikingly different pathways due to the shape selectivity and molecular diffusional (traffic control)<sup>3</sup> characteristics of radicals on the zeolite surfaces. The *p*-ACOB is adsorbed on the internal surface, because the *p*-A moiety has access to the zeolite internal structure. Depending on the sorption into the framework, photolysis product distributions of *o*-ACOB can be dramatically varied. The different photochemical results are the consequence of the diffusional and chemical dynamics available to the radicals produced by homolytic photochemical cleavage of the ketone. The sieving of radicals relative to surface reaction depends on relative diffusional processes that will be sensitive to zeolite structure and factors such as extent of dehydration. We are currently investigating these aspects of molecular diffusion traffic control of radicals adsorbed on zeolites.

**Acknowledgment.** We at Columbia thank the National Science Foundation for its generous support of this research. We also thank Dr. J. C. Scaiano, National Research Council of Canada, for preprints and discussion of unpublished results and Dr. Edith Flanigen, Union Carbide Corporation, Tarrytown, NY, for helpful discussions and a generous sample of LZ-105.

(12) The small amount of *p*-A-*p*-A and BB observed may be produced by recombination of *p*-A and B radicals on the zeolite surface, from recombination within the framework of radicals generated within the framework, or from recombination on the surface of radicals generated within the framework following their migration to the surface. The inability of isooctane to extract products lends further evidence to their generation within the zeolite framework.

(13) The *o*-AB formed on the exterior must be accompanied by *o*-A-*o*-A. 100 parts *o*AB corresponds to 50 parts each of *o*-A-*o*-A and BB. As such, approximately 67% of the product distribution for LZ-105 is the result of B· radical sieving.

(14) For the example given in Table I, assuming the *o*-A-*o*-A observed is from the surface photolysis, the internal contribution to the product distribution is approximately 33%.

## Triplet Energy Transfer as a Probe of Surface Diffusion Rates: A Time-Resolved Diffuse Reflectance Transient Absorption Spectroscopy Study

Nicholas J. Turro,\* Matthew B. Zimmt, and Ian R. Gould

Department of Chemistry, Columbia University  
New York, New York 10027

Walter Mahler

Contribution No. 3781, Central Research Department  
E. I. du Pont de Nemours and Co.  
Wilmington, Delaware 19898

Received March 15, 1985

The importance of molecular diffusion to surface photochemistry has been well established.<sup>1</sup> However, no direct measurements of surface diffusion rates have been reported nor have any correlations been established between molecular structure and rates of diffusion. Extraction of diffusion rate constants from fluorescence quenching experiments is complicated by contributions from resonant energy transfer.<sup>2</sup> Triplet energy transfer proceeds via an exchange mechanism, which requires direct overlap of donor and acceptor orbitals.<sup>3</sup> In homogeneous solution, exothermic transfer occurs at diffusion-controlled rates.<sup>3</sup> The rate constant of triplet energy transfer between surface adsorbed molecules should provide a lower bound for surface diffusion. We report the first time-resolved measurements of triplet energy transfer on silica surfaces, employing time-resolved diffuse reflectance transient absorption spectroscopy.<sup>4</sup>

Irradiation (Excimer laser, 351 nm, 20-ns fwhm, <10 mJ) of benzophenone (BZP 10<sup>-5</sup>-10<sup>-4</sup> mol/g of silica) adsorbed on 22, 95, or 255 Å silicas<sup>5</sup> yield transient absorption spectra with maxima at 520 nm<sup>6</sup> (Figure 1). The transient decay on 255 Å silica is exponential with a lifetime of 1.2 μs and is quenched by O<sub>2</sub> and butadiene with rate constants of (4.5 ± 0.1) × 10<sup>4</sup> and (5.0 ± 0.2) × 10<sup>7</sup> torr<sup>-1</sup> s<sup>-1</sup>. On 22 and 95 Å silicas, the decays are nonexponential with first half-lives of 1-2 and 3-5 μs. We assign this transient to the triplet state of benzophenone, <sup>3</sup>BZP\*, by comparison with previous homogeneous solution<sup>7</sup> and surface studies.<sup>4a</sup>

The transient spectra and decays resulting from irradiation of coadsorbed BZP and naphthalene, NP, are very different. The initial transient signal size observed at 520 nm (410 nm) decreases (increases) with increasing NP loading. The transient decays at 520 nm, on 95 and 255 Å silicas, are exponential for NP loadings ≥ 6 and 2 μmol/g, respectively; the decay rate constants increase with NP loading (Figure 2). At the lowest NP loading, the decay half-life at 410 nm is 30 μs.<sup>8</sup> The transient absorption spectrum observed, after <sup>3</sup>BZP\* decays exhibits a maximum at 410 nm

(1) (a) de Mayo, P.; Natarajan, L. V.; Ware, W. R. *Chem. Phys. Lett.* **1984**, *107*, 187. (b) Bauer, R. K.; Borenstein, R.; de Mayo, P.; Okada, K. K.; Rafalska, M.; Ware, W. R.; Wu, K. C. *J. Am. Chem. Soc.* **1982**, *104*, 4635. (c) Beck, G.; Thomas, J. K. *Chem. Phys. Lett.* **1983**, *94*, 553. (d) Turro, N. J.; Cheng, C.-C.; Mahler, W. *J. Am. Chem. Soc.* **1984**, *106*, 5022.

(2) (a) Even, U.; Rademann, K.; Jortner, J.; Manor, N.; Reisfeld, R. *Phys. Rev. Lett.* **1984**, *52*, 2164. (b) Klafter, J.; Blumen, A. *J. Chem. Phys.* **1984**, *80*, 875.

(3) (a) Sandros, K.; Backstrom, H. L. *J. Acta Chem. Scand.* **1962**, *16*, 958. (b) Wilkinson, F. *Adv. Photochem.* **1964**, *3*, 241. (c) Ternin, A. N.; Ermolaev, V. L. *Trans. Faraday Soc.* **1956**, *52*, 1042. (d) Smaller, B.; Avery, E. C.; Remko, J. R. *J. Chem. Phys.* **1965**, *43*, 922.

(4) Wilkinson, F.; Willsher, C. J. *Chem. Phys. Lett.* **1984**, *104*, 272. (b) Kessler, R. W.; Krablicher, G.; Uhl, S.; Oelkrug, D.; Hagan, W. P.; Hyslop, J.; Wilkinson, F. *Opt. Acta* **1983**, *30*, 1099.

(5) 22, 95, and 255 Å silicas have surface areas of 888, 571, and 78 m<sup>2</sup>/g.<sup>14a,b</sup> The number is the average pore diameter in angstroms. The first two silicas are fibrous. The latter is aggregated. Samples were made by adsorption from pentane followed by slow solvent evaporation and evacuation to 1 mtorr.

(6) Signals are analyzed as ΔR/R; R is the reflected light intensity.<sup>4</sup> Decays are quoted as exponential when log (ΔR/ΔR<sub>0</sub>) vs. t is linear for >3 half-lives.

(7) (a) Topp, M. R. *Chem. Phys. Lett.* **1975**, *32*, 144. (b) Beckett, A.; Porter, G. *Trans. Faraday Soc.* **1963**, *59*, 2038.

(8) Irradiation of NP adsorbed without BZP produces no transients.

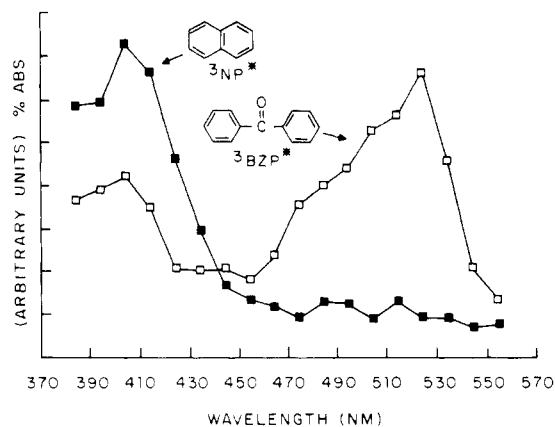


**Figure 1.** (□) Transient absorption spectrum obtained from irradiation of benzophenone on 95 Å silica 400 ns after the pulse. (■) Transient absorption spectrum obtained from irradiation of benzophenone and naphthalene on 95 Å silica 5 μs after the pulse.

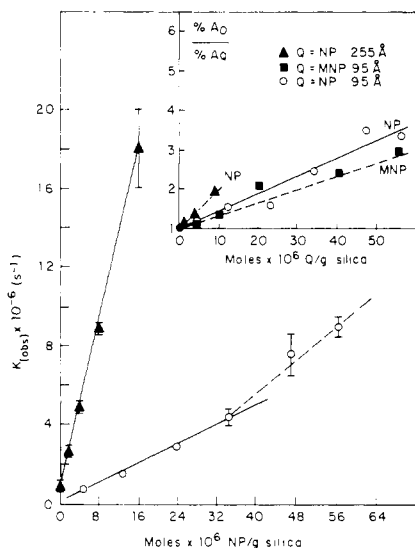


**Figure 2.** Plot of the benzophenone triplet decay rate in the presence of naphthalene (▲) on 255 Å silica and (○) on 95 Å silica. Inset—Ratio of the initial signal size observed at 520 nm in the absence of quencher, % $A_0$ , to that in the presence of quencher, % $A_Q$ . Maximum loading for each surface is 5%.

(Figure 1). We assign this spectrum to the triplet state of naphthalene,  $^3\text{NP}^*$ .<sup>9</sup> The decrease (increase) in the initial signal size at 520 nm (410 nm) is attributed to “static” triplet energy transfer from  $^3\text{BZP}^*$  to NP. The decreased lifetime of  $^3\text{BZP}^*$  is attributed to “dynamic” energy transfer to NP.

Coadsorption of 1-methoxynaphthalene (MNP) and BZP on 95 Å silica also decreases the initial signal size at 520 nm. The decay of  $^3\text{BZP}^*$  is unaltered even at the highest MNP loadings. “Static” triplet energy transfer from  $^3\text{BZP}^*$  to MNP occurs, but “dynamic” energy transfer is too slow to be observed.

Three processes may contribute to the “dynamic” energy transfer to NP: (1) Triplet energy transfer at a distance with no molecular diffusion on the time scale of the  $^3\text{BZP}^*$  lifetime, (2) NP desorption, gas-phase diffusion, readsorption, and collision-induced energy transfer, and (3) NP surface diffusion and collision induced energy transfer. The transfer at a distance mechanism, which is common in singlet energy transfer, can make only a minor contribution to the rate since (a) intramolecular triplet energy transfer between chromophores separated by 15–20 Å occurs with rate constants less than  $100 \text{ s}^{-1}$ <sup>10</sup> (at 25 μm of NP/g of 95 Å silica

the average  $^3\text{BZP}^*$ –NP separation is 23 Å,<sup>11</sup> but the observed transfer rate is  $3 \times 10^6 \text{ s}^{-1}$ , 4 orders of magnitude greater) and (b) NP and MNP quench  $^3\text{BZP}^*$  at diffusion-controlled rates in homogeneous solution,<sup>12</sup> and both quench  $^3\text{BZP}^*$  on silica as evidenced by the “static” energy transfer. The rate constants for energy transfer to NP and MNP by this mechanism should be similar. Since no “dynamic” transfer to MNP is observed, the contribution of the transfer at a distance mechanism is small.

The NP desorption process must also contribute little. Specific heats of adsorption to silica for aromatics and ethers range from 8 to 15 kcal/mol.<sup>13</sup> At 20 °C, there is insufficient NP in the gas phase to contribute significantly to the observed quenching.

The dynamic quenching can, thus, be attributed to collision-induced energy transfer resulting from NP surface diffusion. Previous studies have indicated that aromatics readily diffuse when adsorbed to silica.<sup>1</sup> The absence of dynamic energy transfer in the BZP–MNP system indicates that both BZP and MNP do not diffuse on the time scale of this experiment. This is readily understood since both compounds are Lewis bases which form strong, localized interactions between the oxygen and the surface silanols.

For simplicity,<sup>14</sup> if we treat the silica surface as two dimensional and use of the silica surface areas available from  $\text{N}_2$ -BET analyses,<sup>14,15</sup> the bimolecular rate constants calculated for NP quenching of  $^3\text{BZP}^*$  on 95 and 255 Å silica are  $7.3 \times 10^{15}$  and  $8.5 \times 10^{15} \text{ dm}^2/\text{mol s}$ , respectively. Although the physical structure of the 95 and 255 Å silicas are very different, the quenching rate constants are remarkably similar. These values are the first measure of triplet energy transfer rate constants for adsorbed molecules and serve as a lower limit for the diffusion rate constant of NP on silica. Previously, de Mayo estimated a  $k_Q$  for the quenching of acenaphthylene triplet by ferrocene of  $7.0 \times 10^{15} \text{ dm}^2/\text{mol s}$  from a Stern–Volmer analysis of quantum yields.<sup>1b</sup> Contributions from static triplet energy transfer were not included in the analysis. The present study and fluorescence quenching studies by deMayo<sup>1a</sup> show that their exclusion from the analysis can significantly overestimate the dynamic quenching rate constant.

The quencher loading dependence of the static triplet energy transfer is shown in the inset of Figure 2. Transformation to units of percent surface coverage<sup>5</sup> shows that 95 Å silica is 3.2 times more effective in promoting static transfer than is 255 Å silica. On 95 Å silica, NP is >1.6 times more effective than MNP in the static quenching of  $^3\text{BZP}^*$ . The absence of a strong Lewis acid or base site in NP may increase its tendency to absorb adjacent to bound BZP.

In conclusion, we have demonstrated, using time-resolved diffuse reflectance transient absorption spectroscopy, that triplet energy transfer occurs via both static and dynamic pathways on silica. Static transfer is instantaneous on the time scale of our experiments. Rate constants for dynamic transfer, measured for the first time, place a lower limit on the diffusion of naphthalene on silica.

**Acknowledgment.** We at Columbia thank the National Science Foundation and IBM for the generous support of this research. M.B.Z. thanks NSF for a predoctoral fellowship. Helpful discussions with Drs. M. Drake and J. Klafter of Exxon Corporation are gratefully acknowledged.

**Registry No.** Benzophenone, 119-61-9; naphthalene, 91-20-3.

(11) 23 Å is obtained by calculating the average surface area per NP, assuming a flat surface, obtaining the radius of the corresponding circle, and multiplying by  $2/3$ .  $2/3$  is the average distance from a unit circle's center assuming random placement.

(12) MNP quenches  $^3\text{BZP}^*$  with a rate constant of  $1.21 \times 10^{10} \text{ M}^{-1} \text{ s}^{-1}$  in  $\text{CH}_3\text{CN}$ .

(13) Kiselev, A. V.; Koutetski, Y.; Chizhek, I. *Dokl. Phys. Chem. (Engl. Transl.)* **1962**, *147*, 769.

(14) The surface of silica is very irregular and may be of higher dimensionality of two. For a fractal view of silica surfaces see: Farin, D.; Volpert, A.; Avnir, D. *J. Am. Chem. Soc.* **1985**, *107*, 3368.

(15) (a) Mahler, W.; Bechtold, M. *Nature (London)* **1980**, *285*, 27. (b) Brunauer, S.; Emmett, P.; Teller, E. *J. Am. Chem. Soc.* **1938**, *60*, 309.

(9) Kessler, R. W.; Wilkinson, F. *J. Chem. Soc., Faraday, Trans. 1*, **1981**, *77*, 309.

(10) (a) Keller, R. P.; Dolby, L. *J. Am. Chem. Soc.* **1969**, *91*, 1293. (b) Breen, D. E.; Keller, R. A. *J. Am. Chem. Soc.* **1968**, *90*, 1935.